JACS
JOURNAL OF THE AMERICAN CHEMICAL SOCIETY
Communication
pubs.acs.org/JACS

Synthesis of Monoclinic Potassium Niobate Nanowires That Are Stable at Room Temperature

Seungwook Kim,[†] Ju-Hyuck Lee,[‡] Jaeyeon Lee,[§] Sang-Woo Kim,[‡] Myung Hwa Kim,[§] Sungnam Park,[#] Haegeun Chung,[∥] Yong-Il Kim,*[,⊥] and Woong Kim*[,†,▽]

[†]Department of Nano-Semiconductor Engineering, [#]Department of Chemistry, and [▽]Department of Materials Science and Engineering, Korea University, Seoul 136-713, Republic of Korea

[‡]School of Advanced Materials Science and Engineering, SKKU Advanced Institute of Nanotechnology (SAINT), Center for Human Interface Nanotechnology (HINT), Sungkyunkwan University (SKKU), Suwon 440-746, Republic of Korea

[§]Department of Chemistry & Nano Science, Ewha Womans University, Seoul 120-750, Republic of Korea

[∥]Department of Environmental Engineering, Konkuk University, Seoul 143-701, Republic of Korea

[⊥]Korea Research Institute of Standards and Science, Daejeon 305-340, Republic of Korea

Supporting Information

ABSTRACT: We report the synthesis of $KNbO_3$ nanowires (NWs) with a monoclinic phase, a phase not observed in bulk $KNbO_3$ materials. The monoclinic NWs can be synthesized via a hydrothermal method using metallic Nb as a precursor. The NWs are metastable, and thermal treatment at ∼450 °C changed the monoclinic phase into the orthorhombic phase, which is the most stable phase of $KNbO_3$ at room temperature. Furthermore, we fabricated energy-harvesting nanogenerators by vertically aligning the NWs on $SrTiO_3$ substrates. The monoclinic NWs showed significantly better energy conversion characteristics than orthorhombic NWs. Moreover, the frequency-doubling efficiency of the monoclinic NWs was ∼3 times higher than that of orthorhombic NWs. This work may contribute to the synthesis of materials with new crystalline structures and hence improve the properties of the materials for various applications.

Alkaline niobates, including $KNbO_3$, are receiving increasing attention because of their excellent nonlinear optical (NLO), piezoelectric, ferroelectric, and photocatalytic properties.[1] For example, $KNbO_3$ is a promising material for optical applications such as optical wave guiding, frequency doubling, and holographic storage.[2] Also, alkaline niobates are prime candidates for Pb-free, environmentally friendly piezoelectric materials to replace currently dominant lead zirconium titanates.[3]

In nanowire (NW) form, the applications of alkaline niobates can be greatly extended to the emerging research fields of nanogenerator-based energy harvesting and nanobiotechnology. For example, Suyal et al.[4] showed that $KNbO_3$-based NWs can be useful elements in nanometric electromechanical devices by measuring their piezoelectric response and polarization switching. On the other hand, Nakayama et al.[5] demonstrated the potential of $KNbO_3$ NWs as tunable NLO probes of scanning microscopy for physical and biological sciences.

Nanowires can have novel characteristics differing from those of the bulk counterpart as a result of their low dimension, providing new opportunities for research and technological development.[6] For example, it has recently been reported that hydrothermally grown $KNbO_3$ NWs have a monoclinic phase that has not been observed in bulk $KNbO_3$.[7] This is remarkable because the low-symmetry phase typically generates phenomenal dielectric and electromechanical responses. To date, however, the monoclinic phase of $KNbO_3$ NWs has been observed only at low temperature ($T \approx 80$ K), impeding investigations and applications of the materials. Therefore, developing new synthetic methods to produce low-symmetry phases of given materials that are stable at room temperature (RT) could be a critical breakthrough for both fundamental research and technological development.

Here we report a novel synthetic route to monoclinic $KNbO_3$ NWs that are stable at RT. The space group ($P1m1$), lattice parameters, and atomic positions of the monoclinic NWs were determined by powder X-ray diffraction (XRD) and neutron powder diffraction (NPD) experiments and Rietveld analysis. Heat treatment of the NWs at 450 °C led to the conversion of the monoclinic phase to the orthorhombic phase. Moreover, we grew vertically aligned $KNbO_3$ NWs on lattice-matched $SrTiO_3$ substrates. The vertically aligned monoclinic NWs showed ∼4 times higher power generation than orthorhombic NWs. Additionally, frequency doubling via second-harmonic generation (SHG) by the NWs was observed upon laser excitation. Our demonstration of a robust synthetic protocol that affords a stable low-symmetry phase of $KNbO_3$ NWs may add a new perspective, especially in the study of piezoelectric materials.

The $KNbO_3$ NWs were synthesized via a hydrothermal reaction using metallic Nb powder. To date, the most widely used route for the synthesis of $KNbO_3$ NWs has been the hydrothermal method using Nb_2O_5 powder as the precursor.[5,7−10] However, NWs produced by this method have an orthorhombic phase at RT. Moreover, in spite of its widespread

Received: August 18, 2012
Published: December 12, 2012

dx.doi.org/10.1021/ja308209m | J. Am. Chem. Soc. 2013, 135, 6−9

use, this method requires a reaction time of ~1 week.[9,10] In our work, we found Nb to be more reactive than Nb_2O_5 in the hydrothermal reaction, allowing monoclinic $KNbO_3$ NWs to be synthesized successfully only in 12 h. In addition, our method produces $KNbO_3$ NWs on a gram scale. Figure 1a shows a vial

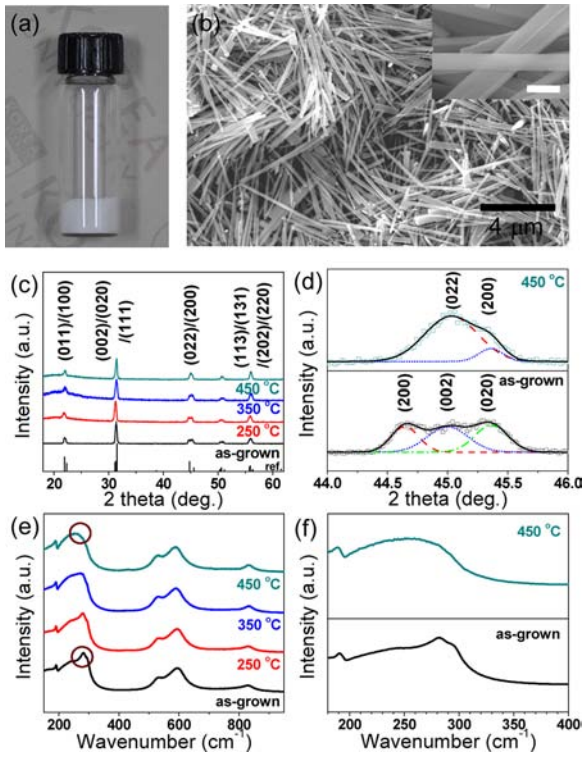

Figure 1. (a) $KNbO_3$ NW powder in a 2 mL vial. (b) SEM image of $KNbO_3$ NWs. The inset shows a high-magnification SEM image (scale bar = 300 nm). (c) XRD patterns of the NWs as grown and after heat treatment at various temperatures (reference data is from JCPDS no. 77-1098). (d) Expanded view of the XRD patterns at 2θ = 44–46° for as-grown and heat-treated (450 °C) NWs. (e, f) Raman spectra of the NWs at (e) 150–950 and (f) 180–400 cm^{-1}.

of the $KNbO_3$ NW powder produced by the Nb-based hydrothermal reaction. The scanning electron microscopy (SEM) image (obtained using a Hitachi S-4800 microscope) clearly shows that the white powder consisted mostly of $KNbO_3$ NWs (Figure 1b). The Figure 1b inset shows that the individual NWs have a square-shaped cross section. The thickness and length of the NWs were 74.0 ± 11.7 nm and 5.1 ± 1.4 μm, respectively (mean ± 1 standard deviation, n = 100). For the synthesis of $KNbO_3$ NWs, Nb powder (Alfa Aesar) and KOH (Sigma-Aldrich) were used as the Nb and K sources, respectively. A 15 M aqueous KOH solution was obtained by dissolving 12.624 g of KOH in 15 mL of deionized water followed by ultrasonication. Subsequently, 0.874 g of Nb powder (~0.63 M) was added to the KOH solution in a 30 mL Teflon-lined stainless steel autoclave. The autoclave was heated to 150 °C, and after 12 h of reaction, it was cooled to RT naturally. NWs in white powder form were obtained by rinsing the product with deionized water and precipitating it with centrifugation for 5 min at 2000 rpm. This rinsing step was repeated until the pH of the solution reached ~7. Finally, the sample was dried at 80 °C overnight. The mass of the final product was >1.2 g, indicating that ~70% of the Nb source was incorporated into the $KNbO_3$ NWs.

The $KNbO_3$ NWs have a monoclinic phase and are metastable at RT. Their crystalline structures were characterized by XRD on a Rigaku D/Max 2500 V/PC diffractometer with Cu Kα radiation (Figure 1c,d) and Raman spectroscopy using a Renishaw inVia spectrometer (Figure 1e,f), which showed the as-grown NWs to have a stable monoclinic phase. Our results are consistent with the data recently reported by Louis et al.[7] for monoclinic $KNbO_3$ NWs observed at low temperature and are clearly different from the data for any phase of bulk $KNbO_3$. Especially, three peaks observed near 45° in the XRD pattern and the sharp peak near 280 cm^{-1} in the Raman spectrum are clearly different from those of the orthorhombic phase (Figure 1c–f). While the monoclinic phase was previously observed at significantly lower temperature (~80 K),[7] a monoclinic phase that is stable at RT was obtained in this work for the first time. In general, bulk $KNbO_3$ materials show multiple phase transitions with changes in temperature: cubic to tetragonal at 435 °C, tetragonal to orthorhombic at 225 °C, and orthorhombic to rhombohedral at −10 °C.[11] Therefore, the orthorhombic phase is the most stable phase of bulk $KNbO_3$ at RT. Consistently, our hydrothermally grown NWs showed the orthorhombic phase after they were heat-treated at 450 °C for 30 min in air and then cooled to RT naturally.

Furthermore, we determined the crystal structure of the monoclinic $KNbO_3$ NWs by NPD, XRD, and Rietveld analysis. As a result, the $P1m1$ space group was assigned to the structure. The lattice parameters were determined to be a = 4.04976(6) Å, b = 3.99218(6) Å, c = 4.02076(7) Å, and β = 90.1012(27)°. Combined Rietveld refinement was carried out using the General Structure Analysis System (R_{wp} = 5.6%, R_p = 3.92%, R_e =3.70%, and $S = R_{wp}/R_e$ = 1.23; for details, see the Experimental Section, Figures S1–S3, and Table S1 in the Supporting Information). Our results clearly verified the monoclinic phase of the NWs. Although it is not completely clear why our synthetic conditions preferentially generate monoclinic NWs over orthorhombic ones, we suspect that the use of the more reactive Nb precursor instead of Nb_2O_5 could be critical. Relative to the Nb_2O_5 precursor, the Nb precursor generated $KNbO_3$ NWs in a shorter reaction time (12 h vs 6 days). The high reactivity of the precursor could lead to a kinetically favored monoclinic phase because of lower activation energy. On the other hand, the thermodynamically favored orthorhombic phase could be obtained if enough energy is applied (e.g., in the form of heat). Indeed, we observed that the metastable monoclinic NWs were transformed into thermodynamically stable orthorhombic NWs upon thermal treatment at ~450 °C. Consistently, it has also been widely reported that various materials with metastable crystal phases can be kinetically prepared using reactive precursors.[12] To determine the crystal structure, XRD analysis was carried out over the scattering angle range 20° ≤ 2θ ≤ 145° with a 2θ step of 0.02° in the reflection geometry using graphite-monochromatized Co Kα radiation (Rigaku, D/Max 2200 V). NPD was performed over the range 0° ≤ 2θ ≤ 160° with a 2θ step of 0.05° at a neutron wavelength of 1.8343 Å on the high-resolution powder diffractometer at the Hanaro Center of the Korea Atomic Energy Research Institute.

Individual $KNbO_3$ NWs were single-crystalline and showed lattice parameters consistent with those obtained from the Rietveld refinement. The crystal structures of the individual NWs were investigated by high-resolution transmission electron microscopy (HRTEM; FEI Tecnai G2 F30 micro-

dx.doi.org/10.1021/ja308209m | J. Am. Chem. Soc. 2013, 135, 6–9

scope) and selected-area diffraction (SAED) (Figure 2). Lattice fringes were clearly observed on both the monoclinic and orthorhombic NWs. The lattice fringe spacings and diffraction patterns indicated that monoclinic NWs can grow along the [100], [010], and [001] directions (Figure 2a,b and Figure S4). Orthorhombic NWs with growth directions of both [100] and [011] were observed (Figure 2c,d). Amorphous coatings with a thickness of a few nanometers were found along the NWs by HRTEM (Figure 2a).

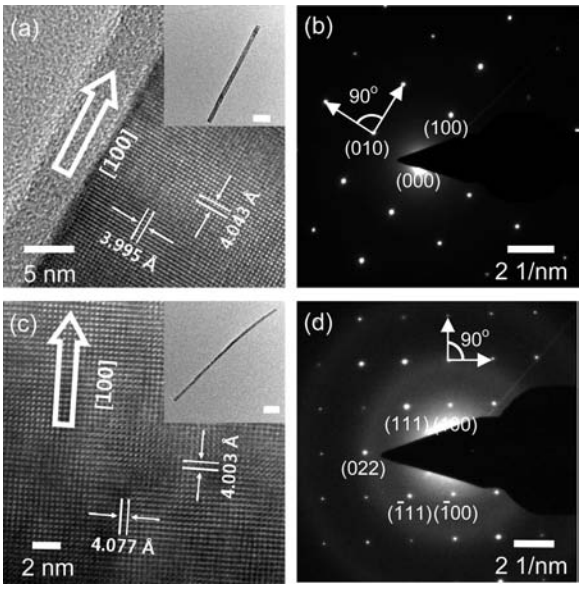

Figure 2. (a) HRTEM image of as-grown monoclinic NWs. The open arrow indicates the growth direction. The inset shows the entire NW (scale bar = 500 nm). (b) Corresponding SAED pattern. (c, d) HRTEM image and SAED pattern of NWs heat-treated at 450 °C.

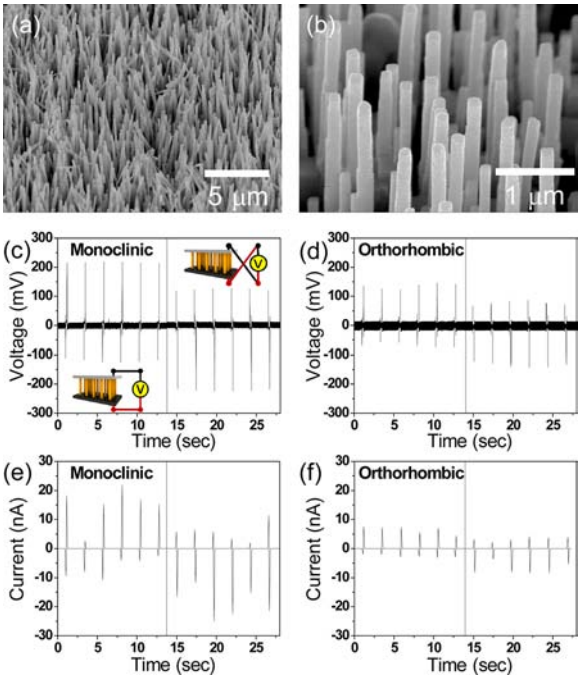

Figure 3. (a) Low- and (b) high-magnification SEM images of $KNbO_3$ NWs grown on Nb-doped $SrTiO_3$ substrates. (c, d) Output voltages and (e, f) output currents of nanogenerators based on (c, e) monoclinic and (d, f) orthorhombic NWs.

$KNbO_3$ NWs were most successfully synthesized at a reaction temperature of 150 °C. The reaction temperature had a significant influence on the yield and morphology of the final $KNbO_3$ product (Figure S5). Although $KNbO_3$ NWs were obtained at 130 °C, the yield of the product was very low. On the other hand, both the yield of the product and the portion of NWs among the product were high at 150 °C. Some NWs were observed in the product synthesized at 170 °C, but the portion of NWs was very low. Only sub-micrometer-scale particulates were observed in the product of the reaction carried out at 190 °C.

Moreover, we showed that $KNbO_3$ NWs can be vertically grown on $SrTiO_3$ substrates. A 0.5 wt % Nb-doped $SrTiO_3$(100) substrate (sheet resistance ≈ 0.2 Ω/sq) with dimensions of 0.5 cm × 0.5 cm was used. The experiment was carried out under the same conditions as described above except that the substrate was suspended using a homemade Teflon structure ∼1 cm above the bottom of the autoclave. $SrTiO_3$(100) was chosen because the lattice parameter of the cubic $SrTiO_3$ crystal (a = 3.905 Å; JCPDS no. 79-0176) is close to the lattice parameters of $KNbO_3$. This close match of the lattice parameters is responsible for the successful growth and vertical alignment of the $KNbO_3$ NWs. Figure 3a,b shows low- and high-magnification SEM images of $KNbO_3$ NWs vertically aligned with respect to the $SrTiO_3$(100) substrate. When the NWs were relatively long, aggregation of the tips of the NWs due to solvent evaporation was observed (Figure 3a). The tips of the NWs were flat and square-shaped (Figure 3b). Further SEM investigation showed that a thin $KNbO_3$ film formed on the $SrTiO_3$ surface and then split into sub-micrometer-scale square islands and finally into NWs (Figures S6 and S7). Moreover, TEM investigation of the $KNbO_3$−$SrTiO_3$ interface showed that the growth was epitaxial (Figure S8). The lattice spacing at the interface was 3.912 Å. This value gradually decreased to 3.904 Å over ∼13 layers down toward the $SrTiO_3$ side and gradually increased to 4.027 Å over ∼24 layers up toward the $KNbO_3$ side. This result indicates that the strain was localized near the $KNbO_3$−$SrTiO_3$ interface (∼15 nm thick).

Nanogenerators fabricated with vertically aligned monoclinic NWs showed superior performance compared with those with orthorhombic NWs (Figure 3c−f). More specifically, the powers of monoclinic- and orthorhombic-NW-based nanogenerators were 178.0 and 36.3 nW/cm^2, respectively. Moreover, the monoclinic NWs showed both higher voltage and current generation. The power was calculated by multiplying the integral areas of the maximum voltage and current output of the devices. Nb-doped $SrTiO_3$ substrates and Kapton films coated with Ti (∼5 nm) and Pt (∼100 nm) layers were used as bottom and top electrodes, respectively, of the vertically aligned NW-based nanogenerators. The generators were tapped by applying a vertical pushing force of 1 kgf (=9.807 N) using a pushing tester (Z-Tec Co. Ltd., ZPS-100) with a 1 mm diameter pushing tip.[13] The voltage and current of the nanogenerators were measured using an oscilloscope (Tektronix DPO 3052) and a picoammeter (Keithley 6485), respectively. To confirm that the signal was indeed from the nanogenerators, a switching-polarity test was performed by swapping the polarity of the electrical connections to the nanogenerators (Figure 3c).[14] Our results clearly showed that the monoclinic NWs are superior to orthorhombic NWs for nanogenerator energy harvesting applications. It has been

dx.doi.org/10.1021/ja308209m | J. Am. Chem. Soc. 2013, 135, 6−9

reported that the monoclinic phase is related to a nonconstrained polarization vector and high piezoelectric responses.[7] Further investigation is necessary to evaluate quantitatively the piezoelectric properties of NWs with different phases. Improvement in the energy conversion efficiency of the nanogenerators would also be expected from further optimization of the devices.

Additionally, we observed NLO properties of the $KNbO_3$ NWs by SHG (Figure 4). For this measurement, a thin layer of

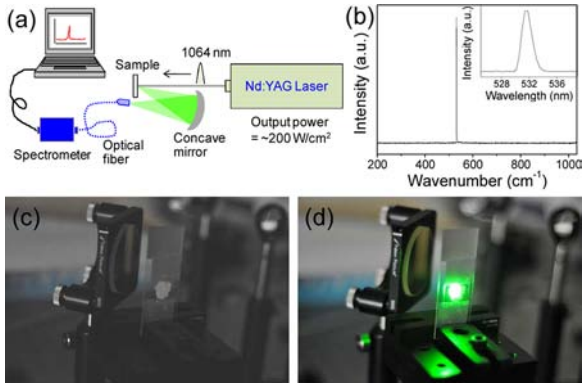

Figure 4. (a) Schematic of the experimental setup for SHG by $KNbO_3$ NWs. (b) Emission spectrum of $KNbO_3$ NWs illuminated with a Nd:YAG laser (λ = 1064 nm). (c, d) Photographs of $KNbO_3$ NWs placed on a glass slide taken with the laser (c) off and (d) on.

$KNbO_3$ NW powder was placed between a slide glass and a cover glass. The layer thickness was a few hundred micrometers. The sample was illuminated at 1064 nm using a commercial Nd:YAG laser (Continuum, Powerlite Precision II 8000), and the emission spectrum from the sample was collected using a spectrometer (Figure 4a). In the emission spectrum, the second harmonic of the 1064 nm laser radiation clearly peaked at 532 nm, indicating the frequency-doubling capability of the $KNbO_3$ NWs (Figure 4b). Interestingly, we observed that the SHG efficiency of the monoclinic NWs was ~3 times higher than that of orthorhombic NWs (Figures S9 and S10). Figure 4c,d shows photographs of the $KNbO_3$ NW sample taken with the laser off and on, respectively. Bright green light (532 nm) was generated from the sample upon laser irradiation. This result indicates that the $KNbO_3$ NWs produced from our current method have decent quality and show the expected NLO properties.[5]

In summary, high-quality monoclinic $KNbO_3$ nanowires were synthesized via a hydrothermal method using Nb powder as a precursor. The monoclinic NWs were stable at room temperature and changed into the orthorhombic phase after heat treatment at 450 °C. Moreover, vertically aligned NWs were successfully synthesized on $SrTiO_3$ substrates and integrated into nanogenerators, where the monoclinic NWs showed superior energy conversion characteristics compared with orthorhombic NWs. In addition, the SHG efficiency for the monoclinic NWs was ~3 times higher than that of orthorhombic NWs. The facile and robust synthesis of the monoclinic $KNbO_3$ NWs presented here may stimulate research on alkaline niobate NWs for a variety of applications, including energy harvesting and nanobiotechnology.

■ ASSOCIATED CONTENT

Supporting Information

Experimental details, additional results, and a CIF. This material is available free of charge via the Internet at http://pubs.acs.org.

■ AUTHOR INFORMATION

Corresponding Author

woongkim@korea.ac.kr; yikim@kriss.re.kr

Notes

The authors declare no competing financial interest.

■ ACKNOWLEDGMENTS

We acknowledge Prof. Brahim Dkhil for providing the crystallographic data for $KNbO_3$ NWs produced in his group. This research was supported by the Fusion Research Program for Green Technologies through the National Research Foundation of Korea (2012-0006183) and the the New & Renewable Energy Technology Development Program (KETEP-20113020010050). S.-W.K. acknowledges financial support by the Basic Science Research Program through the NRF, MEST (2010-0015035).

■ REFERENCES

(1) Dutto, F.; Raillon, C.; Schenk, K.; Radenovic, A. *Nano Lett.* **2011**, *11*, 2517.
(2) Lu, C. H.; Lo, S. Y.; Lin, H. C. *Mater. Lett.* **1998**, *34*, 172.
(3) Saito, Y.; Takao, H.; Tani, T.; Nonoyama, T.; Takatori, K.; Homma, T.; Nagaya, T.; Nakamura, M. *Nature* **2004**, *432*, 84.
(4) Suyal, G.; Colla, E.; Gysel, R.; Cantoni, M.; Setter, N. *Nano Lett.* **2004**, *4*, 1339.
(5) Nakayama, Y.; Pauzauskie, P. J.; Radenovic, A.; Onorato, R. M.; Saykally, R. J.; Liphardt, J.; Yang, P. D. *Nature* **2007**, *447*, 1098.
(6) (a) Xia, Y. N.; Yang, P. D.; Sun, Y. G.; Wu, Y. Y.; Mayers, B.; Gates, B.; Yin, Y. D.; Kim, F.; Yan, Y. Q. *Adv. Mater.* **2003**, *15*, 353. (b) Kuykendall, T.; Pauzauskie, P. J.; Zhang, Y. F.; Goldberger, J.; Sirbuly, D.; Denlinger, J.; Yang, P. D. *Nat. Mater.* **2004**, *3*, 524. (c) Choi, H. J.; Seong, H. K.; Chang, J.; Lee, K. I.; Park, Y. J.; Kim, J. J.; Lee, S. K.; He, R. R.; Kuykendall, T.; Yang, P. D. *Adv. Mater.* **2005**, *17*, 1351. (d) Wu, B.; Heidelberg, A.; Boland, J. J. *Nat. Mater.* **2005**, *4*, 525. (e) Lu, W.; Lieber, C. M. *Nat. Mater.* **2007**, *6*, 841. (f) Boukai, A. I.; Bunimovich, Y.; Tahir-Kheli, J.; Yu, J. K.; Goddard, W. A., III; Heath, J. R. *Nature* **2008**, *451*, 168. (g) Hochbaum, A. I.; Chen, R. K.; Delgado, R. D.; Liang, W. J.; Garnett, E. C.; Najarian, M.; Majumdar, A.; Yang, P. D. *Nature* **2008**, *451*, 163. (h) Nam, Y. S.; Magyar, A. P.; Lee, D.; Kim, J. W.; Yun, D. S.; Park, H.; Pollom, T. S.; Weitz, D. A.; Belcher, A. M. *Nat. Nanotechnol.* **2010**, *5*, 340.
(7) Louis, L.; Gemeiner, P.; Ponomareva, I.; Bellaiche, L.; Geneste, G.; Ma, W.; Setter, N.; Dkhil, B. *Nano Lett.* **2010**, *10*, 1177.
(8) Vasco, E.; Magrez, A.; Forro, L.; Setter, N. *J. Phys. Chem. B* **2005**, *109*, 14331.
(9) Magrez, A.; Vasco, E.; Seo, J. W.; Dieker, C.; Setter, N.; Forro, L. *J. Phys. Chem. B* **2006**, *110*, 58.
(10) Ding, Q. P.; Yuan, Y. P.; Xiong, X.; Li, R. P.; Huang, H. B.; Li, Z. S.; Yu, T.; Zou, Z. G.; Yang, S. G. *J. Phys. Chem. C* **2008**, *112*, 18846.
(11) Hewat, A. W. *J. Phys. C: Solid State Phys.* **1973**, *6*, 2559.
(12) (a) Li, S. J.; Zhao, Z. C.; Liu, Q. H.; Huang, L. J.; Wang, G.; Pan, D. C.; Zhang, H. J.; He, X. Q. *Inorg. Chem.* **2011**, *50*, 11958. (b) Norako, M. E.; Greaney, M. J.; Brutchey, R. L. *J. Am. Chem. Soc.* **2012**, *134*, 23. (c) Gopalakrishnan, J. *Chem. Mater.* **1995**, *7*, 1265.
(13) Park, H. K.; Lee, K. Y.; Seo, J. S.; Jeong, J. A.; Kim, H. K.; Choi, D.; Kim, S. W. *Adv. Funct. Mater.* **2011**, *21*, 1187.
(14) Lee, M.; Bae, J.; Lee, J.; Lee, C. S.; Hong, S.; Wang, Z. L. *Energy Environ. Sci.* **2011**, *4*, 3359.